

Two-photon resonant effect of hyper-Raman scattering in the vicinity of the direct forbidden gap in a rutile crystal

Kenji Watanabe and Kuon Inoue

Research Institute of Applied Electricity, Hokkaido University, Kita-ku, Sapporo 060, Japan

(Received 16 January 1990)

A two-photon resonance effect of the hyper-Raman scattering from optic phonons was investigated in a rutile crystal at 30 K near the direct forbidden energy gap E_g . The scattering efficiency of the allowed modes in the 90° scattering geometry was found to increase remarkably, as twice the incident photon energy, $2\hbar\omega_i$, approaches E_g from below. The result can be reasonably interpreted in terms of a two-photon ingoing resonance with E_g . Further, the forbidden LO mode in the backward-scattering geometry was also found to show a sharp two-photon resonant behavior at the band edge. The origin may be attributed to resonance with the excitons due to the \mathbf{q} -dependent Fröhlich interaction.

Because its selection rules differ from those of Raman scattering, hyper-Raman scattering has been used as a new spectroscopic method for obtaining direct information about the Raman-forbidden optic-phonon mode.¹⁻³ For example, it is established as an important method for studying Raman-forbidden soft modes^{4,5} in structural phase transitions. Experimentally, hyper-Raman scattering is in principle very simple as is Raman scattering. To date, almost all experiments have been performed using a Q -switched Nd-yttrium aluminum garnet (YAG) laser of $1.06\ \mu\text{m}$ wavelength and for a material that is transparent for incident and scattered photons with energy $\hbar\omega_i$ and $\hbar\omega_s$, respectively. Hyper-Raman signals are generally very weak in those experiments, and consequently, measurements have been restricted to those materials for which the signal is relatively intense. Therefore, it is undoubtedly important to improve the sensitivity so as to make this spectroscopy more useful. One possibility might be to utilize a resonant enhancement of the signal.

The purpose of this paper is to confirm that this enhancement occurs when twice the incident photon energy $2\hbar\omega_i$ falls close to the band-gap energy E_g of the solid. We are also concerned with resonant effects in both the allowed and forbidden hyper-Raman scattering by phonons in solids in a similar sense to those in the Raman scattering;^{6,7} in the hyper-Raman scattering we should expect to observe the resonant effects when the value $2\hbar\omega_i$ (or $\hbar\omega_s$) almost coincides with the energy of the specific optical transition, instead of $\hbar\omega_i$ in the Raman scattering. We recently reported a resonant enhancement of hyper-Raman efficiency in SrTiO_3 .^{8,9} However, the interpretation of the result was not necessarily clear because of the indirect nature of the band gap together with the ambiguous location of the lowest direct gap.

In this paper we report a two-photon resonant phenomenon in a rutile crystal (TiO_2), which is suited to the present purpose; the lowest direct band gap of TiO_2 (D_{4h}^{14}) having an inversion symmetry is known to be one-photon-absorption forbidden^{10,11} but two-photon-absorption allowed, and thereby the sample is almost transparent for scattered light in the vicinity of the gap. Thus, we should expect the two-photon resonance effect to occur around E_g .

Two rectangular parallelepiped samples were cut from colorless single crystals with two planes parallel to the c axis. The surfaces were polished to be optically flat. The measurement was performed by the ordinary one-beam excitation technique using a homemade repetitively pulsed dye laser pumped by a Cu-vapor laser. The dye laser had characteristics of 3-kW peak power, 20-ns pulse duration, and 6-kHz repetition rate. A dye, styryl-9 was used to cover a near-infrared region from 843 to 780 nm (1.47 to 1.59 eV) which lies in the vicinity of half the band-gap energy ($E_g = 3.034$ eV at 30 K) of rutile.¹⁰

First, we describe the result of the 90° scattering experiment, where the transverse (TO) and longitudinal (LO) optic phonons of E_u symmetry, and the TO phonon of A_{2u} symmetry are allowed. A laser beam polarized parallel ($\mathbf{e}_i \parallel c$) or perpendicular ($\mathbf{e}_i \perp c$) to the c axis was used to irradiate a sample using a lens with a focal length of $f = 3$ cm. The scattered radiation was collected and focused with a lens on the slit of a single-grating monochromator ($F = 4.4$), and was detected with a gated optical-multichannel detector cooled down to -35°C to reduce thermal noise.¹² The accumulation time for observing one spectrum was 30 min. The sample mounted on the holder of a He-gas flow-type cryostat was cooled to 30 K. In Fig. 1(a) an example of the Stokes hyper-Raman spectra for 827 nm (1.50 eV) excitation is shown. The observed lines were assigned labels on the basis of detailed measurements including polarization and temperature dependence.¹³

Variation of the normalized scattering efficiency¹⁴ S/I_L (where I_L refers to the incident laser power flux) with incident photon energy was measured in detail for the respective phonon modes in both $x'(zz,o)z$ and $x'(y'y',o)z$ geometries, where x' and y' , and o denote $\langle 110 \rangle$ and $\langle \bar{1}10 \rangle$, and unpolarized directions, respectively. The result for the E_u - A_{2u} oblique LO mode at $810\ \text{cm}^{-1}$ is shown in Fig. 2 for the two polarization cases. Because this mode has the highest frequency shift, the measurement could be carried out in the widest frequency region with respect to $2\hbar\omega_i$, i.e., beyond the band gap, where the signal gradually suffered the phonon-assisted absorption caused by the indirect band gap. It is noted that although the behavior of this mode is most typical, the trend of the variation,

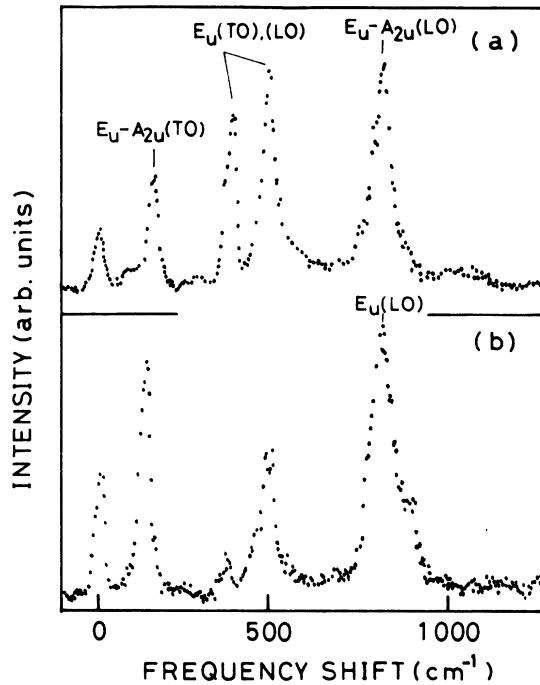


FIG. 1. Examples of the Stokes hyper-Raman spectrum at 30 K in the (a) 90° and (b) backward-scattering geometries for dye-laser excitation with 827 and 816 nm wavelengths, respectively, where the abscissa is plotted as a frequency shift from the value of $2\hbar\omega_i$. In (a) where incident polarization e_i is perpendicular to the c axis, two E_u (TO-LO) modes (unresolved) and two oblique TO-LO modes ($E_u - A_{2u}$) are observed as labeled. The respective linewidths are instrumentally limited (30 cm^{-1}). In (b), i.e., in $y(xx, x+z)\bar{y}$, the forbidden E_u (LO) phonon can be clearly seen at 816 cm^{-1} other than the allowed phonons, i.e., A_{2u} (TO) and three E_u (TO) modes. A weak emission line is also observed at 887 cm^{-1} on the shoulder of the forbidden mode.

S/I_L vs $2\hbar\omega_i$, for other modes is basically similar to the result shown in Fig. 2, aside from the absolute efficiency. In plotting the data points, various corrections such as those due to the wavelength dependences of the optical tools were obviously made. The point at 2.32 eV alone was measured using a Q -switched Nd-YAG laser. The relative magnitudes of the signals of the dye laser and Nd-YAG-laser excitations were determined from a normalization procedure using a reference crystal of KI where the frequency dispersion of the efficiency should be reasonably neglected; the intensity of the TO mode in KI was measured relative to that of the mode in TiO_2 for excitations at both 1.16 and 1.48 eV with the same experimental arrangement. In Fig. 2, the absolute scale is obtained by comparing the present data for KI with earlier data.¹⁴

The result shows that the efficiency increases strikingly in both polarizations as $2\hbar\omega_i$ approaches the direct gap E_g , and still increases beyond it, aside from a small peak at 3.030 eV for the case $e_i \perp c$. The peak, though small, corresponds to the $1S$ exciton excitation.

The present behavior in the $e_i \perp c$ case may be explained as arising from a two-photon incoming resonance with the lowest direct gap E_g . The dominant resonant term in the

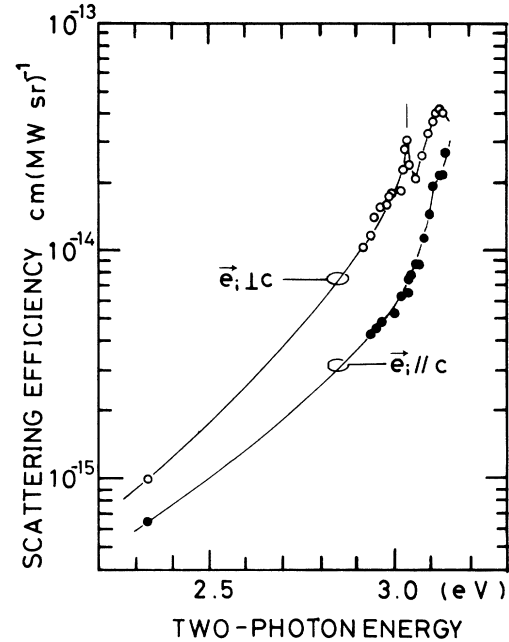


FIG. 2. A plot of the scattering efficiency as a function of $2\hbar\omega_i$ for the allowed LO-oblique phonon with the energy of 810 cm^{-1} for both $e_i \perp c$ and $e_i \parallel c$. The bar indicates the position of the lowest direct-forbidden band gap. The lines are guides to the eye.

hyper-Raman tensor d_{HR} should be described as

$$A[(\hbar\omega_s - E_m)(2\hbar\omega_i - E_1)(\hbar\omega_i - E_n)]^{-1},$$

where A includes a product of matrix elements, i.e.,

$$\langle g | H^{r-e} | m \rangle \langle m | H^{e\text{-ph}} | 1 \rangle \langle 1 | H^{r-e} | n \rangle \langle n | H^{r-e} | g \rangle$$

with H^{r-e} and $H^{e\text{-ph}}$ being electron-radiation and electron-phonon interactions, respectively; $|g\rangle$ and $|i\rangle$, ($i=l, m, n$), denote the ground and intermediate states. The lowest direct-forbidden band transition at 3.034 eV already described corresponds to the excitation from Γ_7^+ valence to Γ_6^+ conduction band^{15,16} and should be reached by a two-photon transition with incident polarizations perpendicular to the c axis. Accordingly, in the case of $e_i \perp c$, the square of the hyper-Raman tensor $|d_{\text{HR}}|^2$ as a function of $2\hbar\omega_i$ may be calculated in terms of a three-band model where the band transition specifying the intermediate states $|1\rangle$ is either $\Gamma_7^+ \rightarrow \Gamma_6^+$ as above or $\Gamma_7^+ \rightarrow \Gamma_6^+$ starting from 3.10 eV as described below, with the bands for the states $|n\rangle$ and $|m\rangle$ being the same. Considering the band structure^{15,16} together with the one-photon absorption data,^{11,17} the most likely intermediate states for $|n\rangle$ and $|m\rangle$ may be those of the degenerate Γ_6^- and Γ_7^- valence band (hole excitation), which lies 1.0 eV below the highest Γ_7^+ band. In Fig. 3, the calculated curve thus obtained is compared to the data points. There, a non-resonant constant term is added to the above two resonant terms before squaring the tensor, and is adjusted in such a manner that the theoretical curve is fitted to the overall data points which are obtained from the observed S/I_L .¹⁴ The result of fitting is rather satisfactory aside from the

slight discrepancy around 3.03 eV. The discrepancy, however, may be improved by taking into account the exciton effect, which will be described elsewhere. Similarly, we could analyze the result for $\mathbf{e}_i \parallel c$ if we have knowledge of the location of the lowest band E_g^{\parallel} which can be reached by two-photon absorption by incident polarization parallel to the c axis. Since there is no information¹⁸ about it, we have recently carried out a two-photon absorption measurement. The result indicates that E_g^{\parallel} is located around 3.10 eV. A most likely assignment for this transition may be an excitation from a spin-orbit-splitting valence band Γ_6^+ to the Γ_6^+ conduction band. Thus, it may be valid to follow a similar procedure as in the case of $\mathbf{e}_i \perp c$ by adopting the above band starting at 3.10 eV as E_g . The fitting is again satisfactory as is seen in Fig. 3.

Next, we briefly describe the result of the backward-scattering geometry, i.e., $y(xx, x+z)\bar{y}$, where all phonons other than three E_u (TO) and one A_{2u} (TO) modes are forbidden to the first-order approximation. The measurement was performed with an experimental procedure similar to the 90° scattering. An example of the spectrum is shown in Fig. 1(b) for 816 nm excitation (1.52 eV). The forbidden E_u -LO phonon line at 816 cm^{-1} was found to be observed with the intensity almost as strong as the other allowed modes. The normalized efficiency S/I_L of the forbidden mode was also measured as a function of $2\hbar\omega_i$. The result of $|d_{\text{HR}}|^2$ shown in Fig. 4 indicates that a sharp resonance manifests itself around 3.030 eV corresponding to the edge of the direct gap.

In what follows, we are concerned with the mechanism of the sharp resonance aside from the whole curve of $|d_{\text{HR}}|^2$ vs $2\hbar\omega_i$. As already described, a second kind of exciton is known to exist with the binding energy of 4 meV for the 1S exciton from a detailed one-photon absorption measurement,^{10,11} where the excitations of the 1S and 2P excitons are weakly optically allowed due to quadrupolar and higher-order dipole transitions, respectively. Having

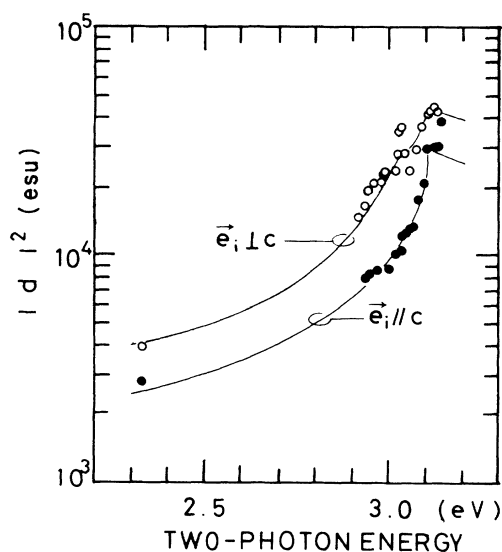


FIG. 3. Comparison of the theoretical curve with the experimental data concerning the magnitude of the squared hyper-Raman tensor for the allowed modes shown in Fig. 2.

the above in mind, the present resonant behavior at 3.030 eV can be interpreted in terms of a simple mechanism where 1S and 2P excitons are predominantly involved as the second and third intermediate states, and the \mathbf{q} -dependent intraband Fröhlich interaction¹⁹⁻²¹ is responsible for the transition between them. This whole process can be shown to satisfy the group-theoretical requirement. The present model may be a two-photon version of the forbidden resonant Raman effect²¹ in a sense that two discrete exciton states predominantly contribute as the intermediate states. The theoretical curve based on this model, the details of which will be presented in a forthcoming paper, is also shown in Fig. 4 for comparison. The agreement is fairly good with reasonable values of parameters. It should be noted that the present process is caused by a quasidouble resonance term such as

$$[(2\hbar\omega_i - \hbar\omega_p - E_g^{\text{ex}})(2\hbar\omega_i - E_g^{\text{ex}})]^{-1},$$

giving rise to a strong two-photon resonance. As for the lower-energy tail below the sharp resonant profile, the mechanism is at present not clear to us, but the one related to the disorder which violates the wave-vector conservation rule to some extent is likely to be involved as is the case²⁰ for the forbidden Raman scattering.

In conclusion, we have presented a clear-cut investigation of the two-photon resonance effect for both allowed and forbidden phonons in hyper-Raman scattering. Particularly, we have found a striking enhancement of the scattering efficiency of the allowed modes in the vicinity of the band gap. This fact will enable one to perform more sensitive hyper-Raman experiments in the future. We

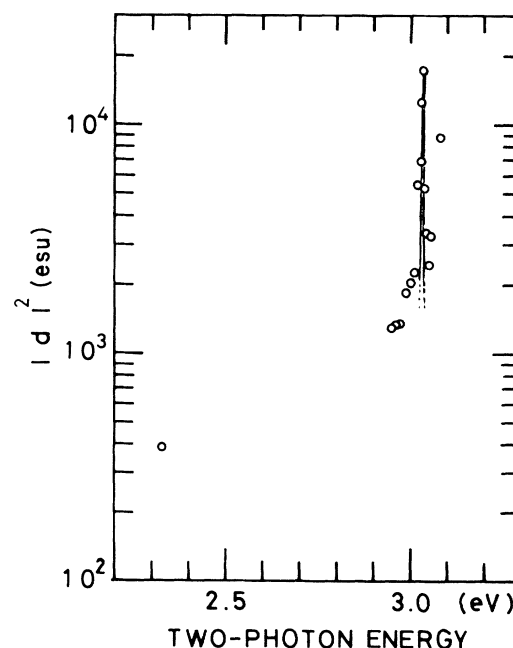


FIG. 4. Variation of the squared hyper-Raman tensor for the forbidden LO modes as a function of $2\hbar\omega_i$. The theoretical curve (solid line) is compared to the experimental data concerning the sharp resonant profile around the band edge. For details, see the text.

also remark that resonant hyper-Raman spectroscopy is a promising technique to unravel specific critical points of band structure, particularly in the ultraviolet region. Note that a photon energy of half the optical transition energy is sufficient.

The authors wish to thank Professor F. Minami for valuable discussions and Dr. A. Yamanaka for help with the experiment. This work was supported by a Grant-in-Aid for Scientific Research from the Ministry of Education, Science and Culture, Japan.

-
- ¹H. Vogt and G. Neumann, *Phys. Status Solidi (b)* **92**, 57 (1979).
- ²K. Inoue and N. Asai, *J. Phys. (Paris) Colloq.* **42**, C6-430 (1981).
- ³H. Vogt and H. Presting, *Phys. Rev. B* **31**, 6731 (1985).
- ⁴See, for example, K. Inoue, *Jpn. J. Appl. Phys.* **24**, Suppl. 24-2, 107 (1985); H. Vogt, *ibid.* **24**, Suppl. 24-2, 112 (1985).
- ⁵K. Inoue, A. Hasegawa, K. Watanabe, H. Yamaguchi, H. Uwe, and T. Sakudo, *Phys. Rev. B* **38**, 6352 (1988).
- ⁶See, for example, A. Pinczuk and E. Burstein, in *Light Scattering in Solids I*, edited by M. Cardona (Springer-Verlag, Berlin, 1983), Chap. 2; R. M. Martin and L. M. Falicov, *ibid.*, Chap. 3.
- ⁷M. Cardona, in *Light Scattering in Solids II*, edited by M. Cardona and G. Guntherodt (Springer-Verlag, Berlin, 1982), Chap. 2.
- ⁸K. Watanabe and K. Inoue, *J. Phys. Soc. Jpn.* **58**, 726 (1989).
- ⁹K. Inoue and K. Watanabe, *Phys. Rev. B* **39**, 1977 (1989).
- ¹⁰J. Pascual, J. Camassel, and H. Mathieu, *Phys. Rev. Lett.* **39**, 1490 (1977); *Phys. Rev. B* **18**, 5606 (1978).
- ¹¹H. Mathieu, J. Pascual, and J. Camassel, *Phys. Rev. B* **18**, 6920 (1978).
- ¹²A. Yamanaka and K. Inoue, *Rev. Sci. Instrum.* **60**, 3253 (1989).
- ¹³K. Watanabe (unpublished).
- ¹⁴H. Vogt, *Phys. Rev. B* **36**, 5001 (1987).
- ¹⁵N. Daude, C. Gout, and C. Jouanin, *Phys. Rev. B* **20**, 5292 (1979).
- ¹⁶J. L. Jourdan, C. Gout, and J. P. Albert, *Solid State Commun.* **31**, 1023 (1979).
- ¹⁷K. Vos and H. J. Krusemyer, *J. Phys. C* **10**, 3893 (1977); K. Vos, *ibid.* **10**, 3917 (1977).
- ¹⁸H. S. Waff and K. Park, *Phys. Lett.* **32A**, 109 (1970).
- ¹⁹R. M. Martin, *Phys. Rev. B* **4**, 3676 (1971).
- ²⁰R. Zeyher, C. S. Ting, and J. L. Birman, *Phys. Rev. B* **10**, 1725 (1974).
- ²¹C. Trallero-Giner, A. Cantarero, and M. Cardona, *Phys. Rev. B* **40**, 4030 (1989).